Agricultural and Forest Meteorology 149 (2009) 976–984

Contents lists available at ScienceDirect

Agricultural and Forest Meteorology

journal homepage: www.elsevier.com/locate/agrformet

Satellite-based estimation of evapotranspiration of an old-growth temperate mixed forest

Junhui Zhang [a], Yanling Hu [a,e], Xiangming Xiao [b], Pengshi Chen [c], Shijie Han [a,*], Guozheng Song [a], Guirui Yu [d]

[a] Institute of Applied Ecology, Chinese Academy of Sciences, 72 Wenhua Road, Shenyang 110016, Liaoning Province, China
[b] Institute for the Study of Earth, Oceans and Space, University of New Hampshire, Durham, NH 03824, USA
[c] Institute of Atmospheric Environment, China Meteorological Administration, Shengyang 110016, China
[d] Institute of Geographic Sciences and Natural Resources Research, Chinese Academy of Sciences, Beijing 100101, China
[e] Graduate School of Chinese Academy of Sciences, Beijing 100039, China

ARTICLE INFO

Article history:
Received 25 March 2008
Received in revised form 28 November 2008
Accepted 5 December 2008

Keywords:
Evapotranspiration
Moderate resolution imaging spectroradiometer (MODIS)
ET-CPT
Water use efficiency (WUE)
Vegetation photosynthesis model (VPM)

ABSTRACT

Evapotranspiration (ET) is a key flux in the water cycle and has strong seasonal dynamics for forest ecosystems. Recently eddy flux covariance measurements are continuously taken at a temperate mixed forest in Northeastern China since 2002. In an effort to better understanding the factors that control the seasonal dynamics of ET, here we (1) calculate ecosystem-level water use efficiency (WUE) from observed water and CO_2 flux data, and (2) relate the resultant WUE with satellite-derived vegetation indices, and (3) develop and evaluate a simple model that uses satellite images and climate data as input data to predict ET on the coupling of photosynthesis and transpiration processes. Ground WUE estimates obtained from eddy covariance tower were correlated with moderate resolution imaging spectroradiometer (MODIS) vegetation indexes (VIs) and ground micrometeorological data over 3 years (2003–2005). The enhanced vegetation index (EVI) was more closely correlated ($r = 0.82$) with WUE than the normalized difference vegetation index (NDVI; $r = 0.64$). Air temperature (T_A) measured over the canopy was the meteorological variable that was most closely correlated with WUE ($r = 0.74$) over years. For the significant correlation between EVI and T_A ($r = 0.82$, $P < 0.05$), EVI was selected as the single variable to predict WUE to simplify calculation. We calculated ET by ET = GPP/WUE, gross primary production (GPP) was predicted by vegetation photosynthesis model (VPM) that uses satellite images and meteorological variables. At a temporal resolution of 8 days, the annual curves showed good correspondence between measured and predicted values of WUE and ET in terms of phase and magnitude for each year. Seasonally integrated predicted ET was +4% (in 2003), +2% (in 2004), +0.4% (in 2005) higher than observed values.

1. Introduction

Evapotranspiration (ET) is the major link between the global energy budgets and hydrological cycles (Smith and Choudhury, 1990), and is a key component of the water budget at a wide range of scales. Accurate monitoring and estimation of ET continuously over large area is the basis for effective spatially resolved water related applications such as management of water resource projects, risk assessments for bushfires, and flooding (Hameed and Mario, 1993; Raupach, 2001). Satellite remote sensing provides routine observations, such as vegetation and land surface temperature, and offers possibilities for extending point measurements or empirical relationships to much larger areas, and many studies have incorporated remote sensing data into ET estimation (Seguin et al., 1994; Kustas and Norman, 1996; Carlson and Buffum, 1989; Allen et al., 2005; Garatuza-Payan and Watts, 2005).

The use of remote sensing models or models coupled with remote sensing is highly recommended to monitor ET over large areas continuously (Verstraeten et al., 2005). Two kinds of approaches have been taken to predict ET from remote sensing data: energy balance-based physical model and empirical model that relate ET to vegetation index (VI) measurements over growing season.

Physical models attempt to predict ET from the surface energy balance equation (Nagler et al., 2005a). Among these models, resistance–surface energy balance model has been widely reported (Cleugh and Dunin, 1995; Hall et al., 1992; Kalma and Jupp, 1990), while its performance has been shown to be unreliable (Cleugh et al., 2007). The Penman–Monteith model provides a more robust approach to estimating land surface evaporation, while its routine

* *Corresponding author*. Tel.: +86 24 83970443.
E-mail address: Hansj@iae.ac.cn (S. Han).

0168-1923/$ – see front matter © 2008 Elsevier B.V. All rights reserved.
doi:10.1016/j.agrformet.2008.12.002

application is always hindered by requiring meteorological forcing data and the aerodynamic and surface resistances (Mauser and Schädlich, 1998; Moran et al., 1996; Cleugh et al., 2007).

Empirical methods utilize the scatter plot between VIs and Ts to derive surface resistance (Price, 1990; Yang et al., 1997; Jiang and Islam, 2001) following the idea of Nemani and Running (1989). However, this requires a continuum of soil moisture (from dry bare soil to saturated bare soil) and vegetation status (from water-stressed full-cover vegetation to well-watered full-cover vegetation) to provide a range of surface conditions. The effects of soil evaporation and vegetation stresses added scatter and uncertainty into the ET estimates (Nagler et al., 2005a). Several researchers tried to explore statistical models using remote sensing to extrapolate eddy covariance water and carbon flux data to regional scales. For example, Wylie et al. (2003) related normalized difference vegetation index (NDVI) to carbon fluxes in a sage-brush-steppe ecosystem, and Nagler et al. (2005a,b) developed an a multivariate regression equation for ET prediction over large reaches of western U.S. rivers by combining remote sensing with flux site measurements with a relative root-mean-square error (RMSE) of 25%. These studies established the potential of using statistical techniques to extrapolate ET measured at eddy covariance flux towers to a regional scale.

Eddy covariance technique is a scale-appropriate way to scale ground measurements of ET and other biophysical processes over larger areas, and to project the results over periods of years, to be used for routine monitoring of regional ecosystems (Running et al., 1999) with relatively minimum uncertainties. It directly measures ET over area possessing longitudinal dimensions ranging between a 100 m and several kilometers (Schmid, 1994) across a spectrum of times scales, ranging from hours to years (Wofsy et al., 1993; Baldocchi et al., 2001). It can provide effective information of ET and biophysical processes which are critical for evaluating ET model and understanding the factors controlling seasonal dynamics of water fluxes (Law et al., 2002).

For vegetation covered area, the close coupling between transpiration and photosynthesis processes is observed (Stanhill, 1986; Steduto et al., 1997; Reichstein et al., 2002; Yu et al., 2008). There are a number of studies of photosynthesis, gross primary production (GPP), and net primary production (NPP) using several methods including measurements, remote sensing, modelling, etc. (Potter et al., 1993; Ruimy et al., 1994; Prince and Goward, 1995; Justice et al., 1998; Xiao et al., 2004a; Turner et al., 2006). GPP often increases with ET across vegetation types. The ratios of GPP to ET, which is defined as water use efficiency (WUE), are similar across vegetation types (Law et al., 2002) and strongly influenced by weather conditions (De Wit, 1958; Tanner and Sinclair, 1983; Law et al., 2002; Abbate et al., 2004; Yu et al., 2008). WUE has been estimated by complex physical model (Gutschick, 2007) or simple meteorology drived empirical models (Wang et al., 2007). There is little report on direct estimation of WUE from satellite images.

In this paper, our objectives are (1) to understand seasonal dynamics of WUE calculated from eddy flux tower data; (2) to develop the quantitative relationship between vegetation indices and WUE, here defined as the ratio of GPP to ET; (3) to predict ET with predicted WUE and GPP estimated from a satellite-based vegetation photosynthesis model (VPM) that uses satellite imagery, air temperature, and photosynthetically actively radiation (PAR; Xiao et al., 2004a,b, 2005), we named as EvapoTranspiration on the Coupling between Photosynthesis and Transpiration (ET-CPT) model. The study site is mature mixed forest ecosystem in Changbai mountain, North-east of China. Flux tower has been established since 2002 in this forest ecosystem and many years of data has been reported (Zhang et al., 2006a,b).

2. Materials and methods

2.1. Study sites and field data

The eddy flux tower site is located in No. 1 Plot at Forest Ecosystem Opened Research Station of Changbai Mountains (128°5′45.79E and 42°24′8.88″ N, Jilin Province, P.R. China), Chinese Academy of Sciences. The annual mean temperature is 0.9–4.0 °C, annual total precipitation is 600–810 mm year^{-1} (evaluated over a period of 20 years). The area is covered by on average 200-year-old, multi-storied, uneven-aged, multi-species mixed forest consisting of Korean pine (*Pinus koraiensis*), *Tilia amurensis*, *Acer mono*, *Fraxinus mandshurica*, *Quercus mongolica* and 135 other species. The mean canopy height is 26 m. A dense understory, consisting of multi-species broad-leaved shrub, has a height of 0.5–2 m. The peak leaf area index is about 6.1. The soil is classified as dark brown forest soil originating from volcanic ashes. The landscape is very flat.

Eddy flux measurements of CO_2, H_2O, energy and routine meteorological variables at this site have been collected since 2002 (Zhang et al., 2006a,b). One open-path eddy covariance measurement system was installed at 40 m on a 62.8 m tower. CO_2/H_2O and wind/temperature fluctuation were measured by Li7500 (IRGA, Li-Cor, USA) open-path CO_2/H_2O sensor and 3D ultrasonic anemometer (CSAT3, Campbell, USA) at 10 Hz rate. Meteorological variables are sampled every 2 s and stored as half-hour statistics (CR23X, Campbell, USA). Meteorological measurements at 40 m include air temperature and relative humidity (HMP45C, Vaisala, Finland), wind speed (A100R, Vector, UK), downward/upward solar radiation and net radiation (CNR1, Kipp and Zonen, The Netherlands), and PAR (Li190SB, Li-Cor, USA). Precipitation (52203, Young, USA) is measured at 62.8 m. Routine QA/QC and corrections, such as planar fit coordinate rotation, frequency response correction, sensors separation correction, influence of humidity on sonic temperature, path correction, WPL correction, etc., were applied to raw eddy flux data. To avoid the underestimation of nighttime fluxes under calm condition, u_* correction was applied to nighttime flux measurements. Upper boundary u_* (UU_*) correction (Zhang et al., 2005) was applied to CO_2 fluxes in winter seasons. The threshold of u_* is 0.17 m s^{-1} for growth period and 0.02 m s^{-1} for dormant seasons. UU_* threshold is 0.37 m s^{-1} (Zhang et al., 2005, 2006a,b). To get annual estimates and time series of CO_2 and ET exchange, artificial neutral network (ANN) technique (Limas et al., 2007) was applied to fill data gaps.

WUE (gC per mm H_2O) here is defined as the ratio of 8-day GPP to ET. 8-Day GPP and ET were derived from half-hourly measurements of CO_2/H_2O fluxes by the eddy covariance technique (Zhang et al., 2006a,b).

2.2. Moderate resolution imaging spectroradiometer (MODIS) data

We downloaded the 8-day land surface reflectance (MOD09-A1) data sets for the period of 2003–2005 from the EROS Data Center, US Geological Survey (http://www.edc.usgs.gov/). Based on the geo-location information (latitude and longitude) of the flux tower site, data of land surface reflectance were extracted from one MODIS pixel that covers the flux tower. Reflectance values of the 8-day land surface reflectance data set from these four spectral bands (blue, red, near infrared (841–875 nm), shortwave infrared (1628–1652 nm) were used to calculate vegetation indices, normalized difference vegetation index, enhanced vegetation index (EVI) and land surface wet index (LSWI, Xiao et al., 2004a). Cloudy observations in a time series of vegetation indices were gap-filled using a simple gap-filling method and the cloud quality flag in the surface reflectance files (Xiao et al., 2003).

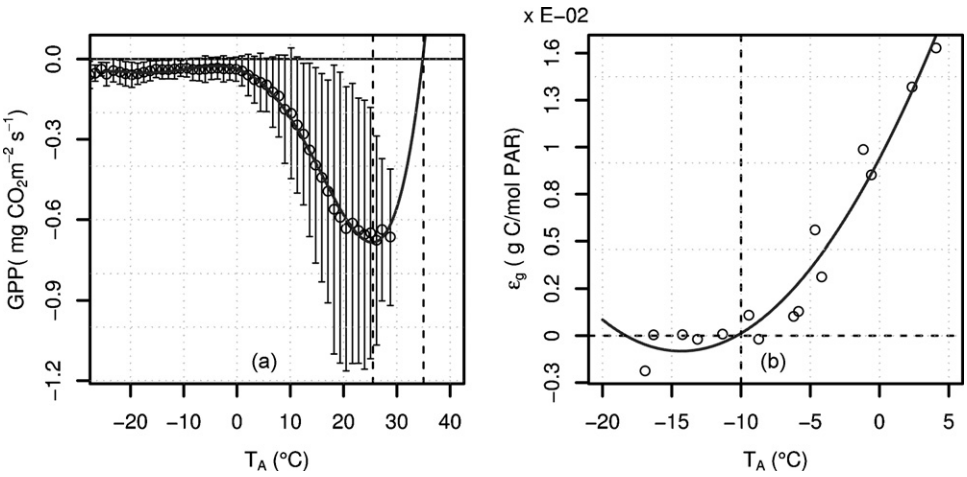

Fig. 1. Temperature response curve of GPP (a) and ε_g (b).

The EVI, NDVI and LSWI are calculated as

$$\mathrm{NDVI} = \frac{\rho_{nir} - \rho_{red}}{\rho_{nir} + \rho_{red}} \tag{1}$$

$$\mathrm{EVI} = 2.6 \times \frac{\rho_{nir} - \rho_{red}}{\rho_{nir} + (6 \times \rho_{red} - 7.5 \times \rho_{blue}) + 1} \tag{2}$$

$$\mathrm{LSWI} = \frac{\rho_{nir} - \rho_{swir}}{\rho_{nir} + \rho_{swir}} \tag{3}$$

where ρ_{swir} is the shortwave infrared reflectance, ρ_{nir} is the near infrared reflectance, ρ_{red} is the red reflectance, and ρ_{blue} is the blue reflectance at the surface.

2.3. ET-CPT model

The ET-CPT model combines water use efficiency and gross primary production to estimate evapotranspiration. In brief, ET is estimated by scaling GPP by WUE as following:

$$\mathrm{ET} = \frac{\mathrm{GPP}}{\mathrm{WUE}} \tag{4}$$

$$\mathrm{WUE} = f(\mathrm{VIs}, T_A, \ldots,). \tag{5}$$

WUE shows strong dependence on weather condition and leaf phenology (De Wit, 1958; Tanner and Sinclair, 1983; Law et al., 2002; Abbate et al., 2004; Gouranga and Harsh, 2007; Yu et al., 2008). To build the function described in Eq. (5), we consequently conducted simple correlation analysis between WUE and vegetation indices, and between WUE and meteorological variables.

GPP is estimated from the vegetation photosynthesis model (Xiao et al., 2004a) as

$$\mathrm{GPP} = \varepsilon_g \, \mathrm{FPAR}_{\mathrm{chl}} \, \mathrm{PAR} \tag{6}$$

where ε_g is the light use efficiency defined as

$$\varepsilon_g = \varepsilon_0 T_{\mathrm{scalar}} W_{\mathrm{scalar}} P_{\mathrm{scalar}} \tag{7}$$

where ε_0 is the apparent quantum yield or maximum light use efficiency and T_{scalar}, W_{scalar}, and P_{scalar} are down-regulation scaling factors for the effects of temperature, water, and leaf phenology on light use efficiency and can be calculated using either surface observational data or remotely-sensed data, respectively.

For this site, ε_g is determined by LAI at seasonal scale and by VPD at peak growth season while LAI and air temperature changed little (Zhang et al., 2006a,b). ε_0 was estimated as the interception of linear relationship between ε_g and VPD on peak growth periods (Zhang et al., 2006b). Value of ε_0 used here is 0.54 gC/mol PAR.

Detailed description of calculation of T_{scalar}, W_{scalar} and P_{scalar} is presented in earlier publications (Xiao et al., 2004a). In calculation of T_{scalar}, T_{min}, T_{opt} and T_{max} values are set to −10, 25 and 35 °C, respectively. These parameters were obtained from GPP–T_A and ε_g–T_A response curves. T_{opt} is the corresponding air temperature to the maximum GPP. The larger root of quadratic GPP–T_A curve was assigned to T_{max} (Fig. 1a). The root of quadratic ε_g–T_A curve was assigned to T_{min} (Fig. 1b) for it's hard to be obtained directly from GPP–T_A curve when air temperature fall down below 0 °C.

3. Results

3.1. Quantitative relationships between WUE and VIs and meteorological variables

We conducted simple correlation analysis between WUE and vegetation indices, and between WUE and meteorological variables (Table 1). WUE was significantly correlated with both NDVI and EVI, but the correlation coefficients were generally higher for EVI than that for NDVI (Table 1 and Fig. 2). One possible reason for this may be that NDVI values were saturated in well-vegetated areas, as the LAI at the old-growth forest site is relatively high (up to 6.1 $m^2\ m^{-2}$), while EVI does not appear to be as saturated as NDVI. T_A was significantly correlated with WUE in general while the r values for WUE on the other meteorological data were not significant (Table 1). WUE followed seasonal EVI and T_A curves more closely than these of NDVI and VPD (Fig. 3).

WUE was regressed against EVI and T_A in a single step. Both EVI and T_A were significant ($P < 0.05$). The proportion of the variability in WUE explained by this equation was 0.69 which is 0.02 and 0.14 lager than single variable equations against EVI (0.67) and T_A (0.55) separately. This may be explained by the significant correlation

Table 1
Correlation coefficients (r) between WUE and VIs, and between WUE and meteorological variables at the tower site by individual years (2003–2005) and by all 3 years (lump together).[a]

Year	EVI	NDVI	VPD	T_A	PAR
2003	**0.84**	**0.75**	−0.01	**0.82**	0.22
2004	**0.78**	**0.68**	−0.47	**0.75**	−0.17
2005	**0.92**	**0.55**	−0.42	**0.76**	0.10
All	**0.82**	**0.64**	−0.19	**0.74**	−0.14

[a] Bold numbers are significant at 0.05 level.

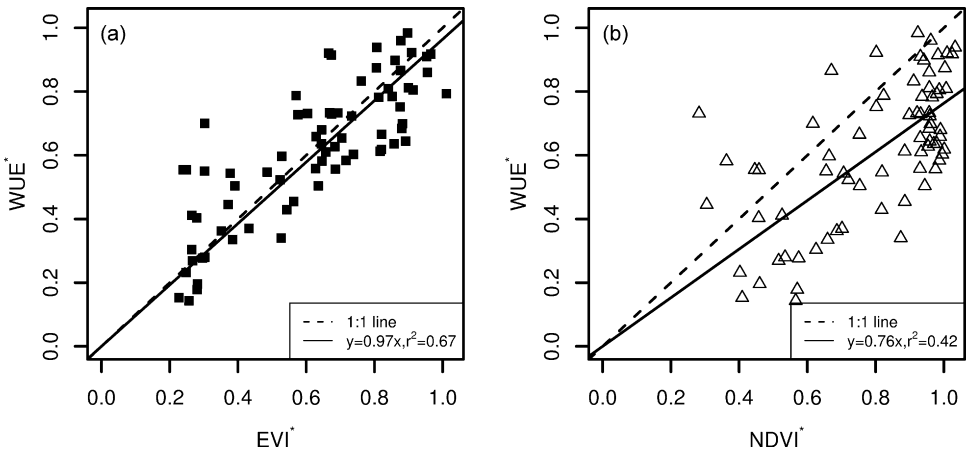

Fig. 2. Simple linear regression of WUE* as a function of EVI* (a) and NDVI* (b). Values are 8-day means over 3 years, 2003–2005. WUE* = WUE/WUE_{max}; EVI* = EVI/EVI_{max}; NDVI* = NDVI/$NDVI_{max}$.

between EVI and T_A ($r = 0.82$, $P < 0.05$). EVI was selected as the single variable to predict WUE to simplify calculation.

Scatter plot of WUE* vs. EVI* is shown in Fig. 2a. Here, WUE* is the scaled WUE as WUE/WUE_{max}. EVI* is the scaled EVI as EVI/EVI_{max}. WUE* was linearly related to EVI*. The equation of best fit is WUE* = 0.97 × EVI* ($R^2 = 0.67$, $P < 0.05$). Assumed WUE* = EVI* which will only produce error of 3%, WUE can then be predicted with following equation:

$$\mathrm{WUE} = \mathrm{EVI}\frac{\mathrm{WUE_{max}}}{\mathrm{EVI_{max}}} \quad (8)$$

In general, predicted WUE agreed well with measured values (Fig. 4).

3.2. Seasonal dynamics of GPP from VPM model

The ET-CPT is built on the coupling of photosynthesis and transpiration processes and uses the water use efficiency and gross primary production to estimate ET. GPP data in this study was estimated with a vegetation photosynthesis model (Xiao et al., 2004a,b, 2005). The validity of VPM at this site is critical to evaluate our research while it previously has been

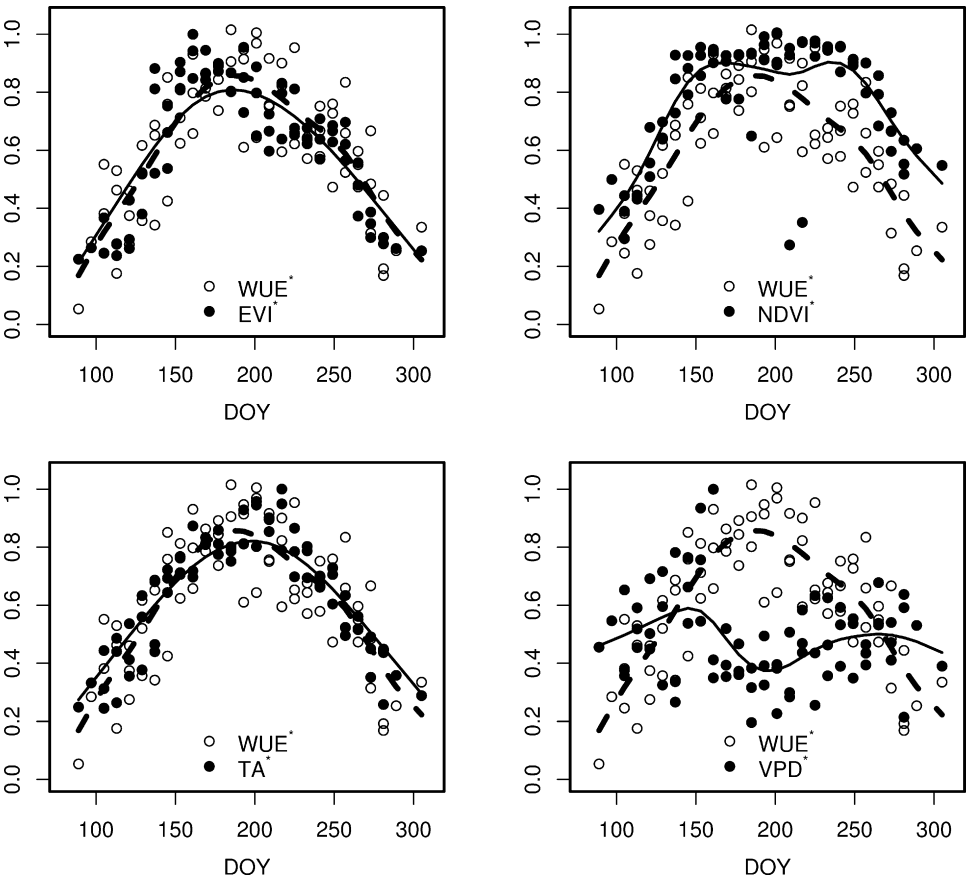

Fig. 3. Seasonal curves for ET, VIs and meteorological variable over 3 years in Changbai broad leaved Korean pine mixed forest. Curves were fit using cubic smoothing spline equations. WUE* = WUE/WUE_{max}; EVI* = EVI/EVI_{max}; NDVI* = NDVI/$NDVI_{max}$; VPD* = VPD/VPD_{max}; $T_A^* = T_A/T_{Amax}$.

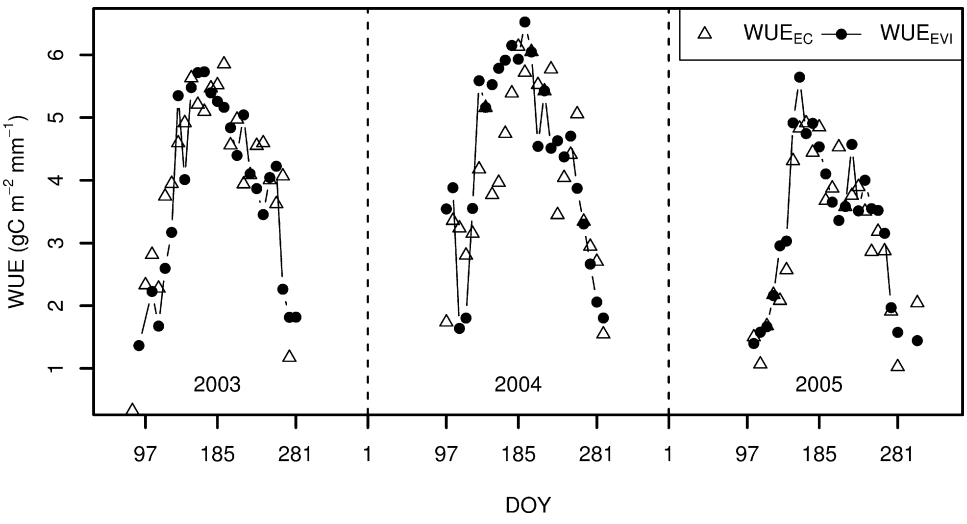

Fig. 4. A comparison of the seasonal dynamics of measured (WUE_{EC}) and predicted (WUE_{EVI}) values for WUE. WUE was predicted from MODIS EVI using Eq. (8).

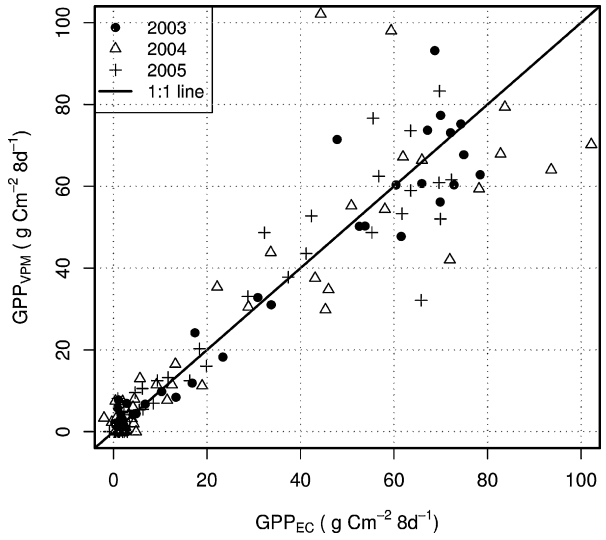

Fig. 5. A linear comparison of predicted and observed GPP (gC m^{-2} $[8d]^{-1}$) at the eddy flux tower site in Changbai broad leaved Korean pine mixed forest, China. The predicted GPP (GPP_{VPM}) is from the VPM model, and observed GPP (GPP_{EC}) is based on the half-hourly data of CO_2 flux from 2003 to 2005 at the flux tower site.

validated over several other ecosystems (Xiao et al., 2004a,b, 2005, 2006).

The VPM-predicted GPP_{VPM} values were compared with eddy flux tower estimates of GPP_{EC} at the flux site. At a temporal resolution of 8 days, GPP_{VPM} agreed well with the eddy covariance measurements GPP_{EC} (Fig. 5, $GPP_{VPM} = 1.02 \times GPP_{EC}$, $R^2 = 0.87$, $P < 0.001$). The annual total GPP_{VPM} values were 1193, 1183, and 1056 gC m^{-2} from 2003 to 2005; and were almost equal to that of flux tower-based GPP_{EC} (1173, 1167, and 1017 gC m^{-2} in three observation years). Their seasonal dynamics were consistent in terms of phase (Fig. 6), though GPP_{VPM} values were generally higher than GPP_{EC} in the early summer, and were lower than GPP_{EC} in the late summer.

3.3. Seasonal dynamics and inter-annual variation of ET from ET-CPT model

Using Eq. (8) and VPM model, we calculated ET values by ET = GPP/WUE, and plotted measured vs. predicted values (Figs. 7 and 8). At a temporal resolution of 8 days, the annual curves showed good correspondence between measured and predicted values in terms of phase and magnitude for each year (Fig. 7). This model successfully replicated trends in ET over years (Fig. 8). The

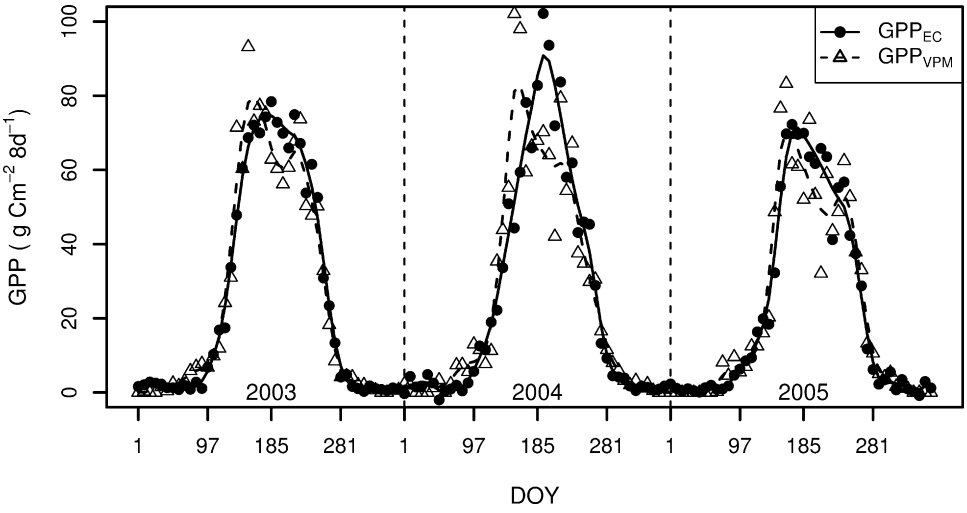

Fig. 6. Seasonal dynamics of measured and predicted GPP (gC m^{-2} $[8d]^{-1}$) at the eddy flux tower site in Changbai broad leaved Korean pine mixed forest, China. The predicted GPP (GPP_{VPM}) is from the VPM model, and observed GPP (GPP_{EC}) is based on the half-hourly data of CO_2 flux from 2003 to 2005 at the flux tower site.

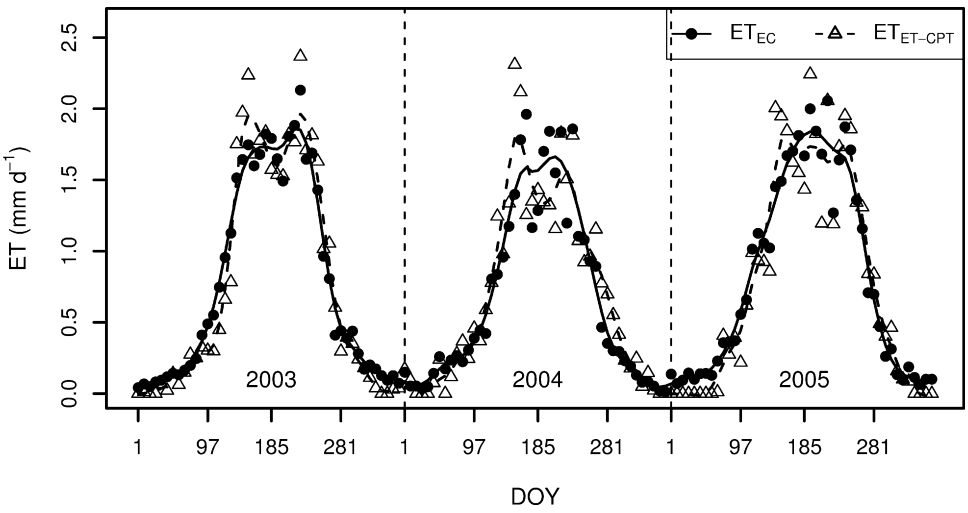

Fig. 7. A comparison of the seasonal dynamics of measured and predicted ET (mm d^{-1}) at the eddy flux tower site in Changbai broad leaved Korean pine mixed forest, China. The predicted ET ($ET_{ET\text{-}CPT}$) is from the ET-CPT model, and observed ET (ET_{EC}) is based on the half-hourly data of ET from 2003 to 2005 at the flux tower site.

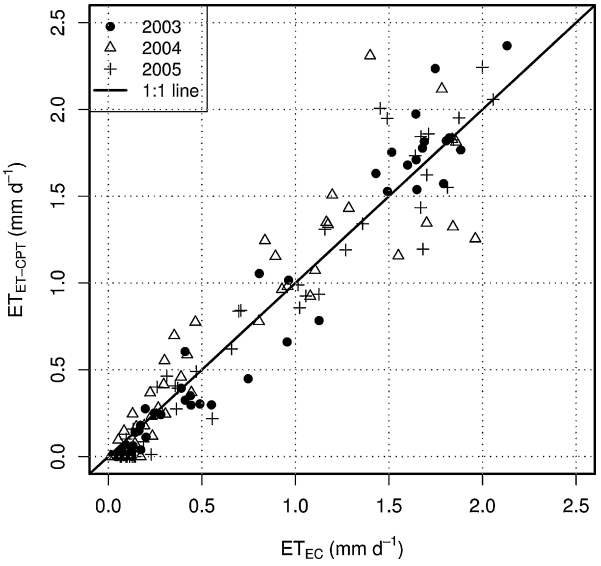

Fig. 8. A linear comparison of predicted and observed ET (mm d^{-1}) at the eddy flux tower site in Changbai broad leaved Korean pine mixed forest, China.

simple linear regression model also shows high correlation between predicted ET and observed ET over years ($ET_{ET\text{-}CPT} = 0.99 \times ET_{EC}$, $R^2 = 0.92$, $P < 0.01$, Fig. 8). Annual integrated $ET_{ET\text{-}CPT}$ was −2% (in 2003), +5% (in 2004), −3% (in 2005) higher than observed values ET_{EC}, respectively (Table 2). In comparison to the seasonally, from May 1 to September 30, integrated ET_{EC} values which accounted for 80% of annual ET_{EC} (Table 2), seasonally integrated $ET_{ET\text{-}CPT}$ was +4% (in 2003), +2% (in 2004), +0.4% (in 2005) higher than observed values, respectively (Table 2).

Table 2
Annual and seasonal (from May 1 to September 30) evapotranspiration measurements by eddy covariance method and estimates by ET-CPT model ($ET_{ET\text{-}CPT}$) (unit: mm).

Year	ET_{EC}		$ET_{ET\text{-}CPT}$	
	ET_{1-12}	ET_{5-9}	ET_{1-12}	ET_{5-9}
2003	286.7	235.1	281.3	244.1
2004	246.2	196.4	257.7	200.9
2005	298.7	237.6	288.9	238.6
Mean	277.2	223.0	275.9	227.9

4. Discussion

4.1. Accuracy of eddy covariance data

Flux measurements require careful calibration to produce reliable data (Rana and Katerji, 2000; Scott et al., 2004). Eddy covariance results reported in this study have been validated in several studies. Wu et al. (2005) compared ET estimate by Bowen-ratio energy balance (BREB) method with corresponding ET measurements by eddy covariance technique. Over a 1 month measurement period, the BREB-based estimates for ET were within 6% of eddy covariance estimates. Diao et al. (2005) and Wang et al. (2005), working at same site using inverse Lagrangian dispersion analysis method, reported a 20% higher ET estimate than eddy covariance measurements over a 5-month period.

Calculation of energy closure ratios is another way to access validity of the eddy covariance estimates. Energy closure ratio for eddy covariance measurements at this site is about 0.79 (Li et al., 2005) which is in the usual range of 0.53–0.99 (Wilson et al., 2002). Based on site-specific information and information from studies in similar conditions elsewhere, error or uncertainty of about 10–20% can be expected for the eddy covariance measurements reported in this study.

4.2. Estimate of WUE

Eq. (8) performed reasonably well to predict dynamics of WUE directly from MODIS-EVI with simpler form. WUE_{MAX} is the only free parameter in Eq. (8). Application of the model to other pixels requires estimation of this parameter (WUE_{MAX}) for individual pixel. It can be obtained from eddy CO_2/H_2O fluxes time series; literatures or historical records where flux measurements are not available. WUE_{MAX} were relatively constant at ecosystem level. According to Law et al. (2002), WUE_{MAX} = 5–6 for rainforest and evergreen conifers, WUE_{MAX} = 7–8 for deciduous broadleaf forests and WUE_{MAX} = 4–6 for crops and grasslands.

4.3. Simulation of ET by ET-CPT

Multi-years simulation with the ET-CPT model shows that, in general, there was a good agreement between $ET_{ET\text{-}CPT}$ and ET_{EC}

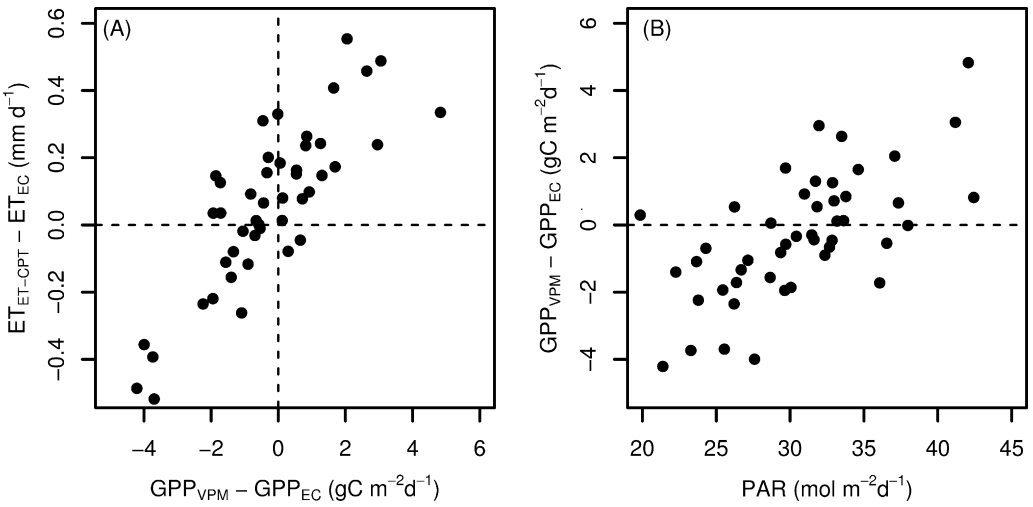

Fig. 9. Dependence of discrepancy in ET predication (ET_{ET-CPT}) and measurements (ET_{EC}) on that in GPP predication (GPP_{VPM}) and measurements (GPP_{EC}) (a); dependence of discrepancy in GPP predication and measurements on photosynthetically actively radiation (PAR, (b)).

during 2003–2005. However, there still exist large differences between ET_{ET-CPT} and ET_{EC} in a few 8-day periods (Fig. 7). Those large discrepancies between ET_{ET-CPT} and ET_{EC} may be attributed to two sources of errors.

The first source is the sensitivity of the GPP predicted by VPM model to PAR and temperature. In some case, over/under-estimation of GPP is attributed to higher/lower input PAR values for the assumed linear relationship between GPP and PAR in VPM model (Fig. 9). PAR varies substantially over space and time. Therefore, improvement in measurement of PAR (both direct and diffusive) at large spatial scale would be substantially benefited. Scenario analysis shows that selection of T_{min} is likely to have some impact on GPP and ET through T_{scalar} (Fig. 10). In this study, we used $T_{min} = -10\ ^{\circ}C$ which minimized errors of annual ET and GPP estimate (Fig. 10) while another process-based ecosystem model used $T_{min} = -2.0\ ^{\circ}C$ for temperate forest (Raich et al., 1991). In the growth period, difference between GPP_{VPM} and GPP_{EC} was minimized when T_{min} was set to $-2.0\ ^{\circ}C$. This 8 °C difference in T_{min} brought difference of 8% in annual ET estimate and 3% of that in growth periods. The difference in optimum T_{min} for whole year and growth period can probably be attributed to the difference in active species composition for this mixed forest.

The second source is the time-series data of vegetation indices derived from satellite images. The compositing method (currently selecting an observation with the maximum NDVI value in a 8-day period) could result in some bias, and one resolution to the issue would be to use daily images as input, although this would requires substantial increases in computer processing (Xiao et al., 2004a). Further investigations are needed to quantify the relative role of individual sources of error in evaluation of the model using ET data from flux tower sites.

In summary, in an effort to better understanding the factors that control the seasonal dynamics of ET, here we (1) calculated ecosystem-level water use efficiency from observed water and CO_2 flux data, and (2) related the resultant WUE with satellite-derived vegetation indices, and (3) developed and evaluated a simple model that uses satellite images and climate data as input data to predict ET on the coupling of photosynthesis and transpiration processes. We find that EVI is strongly correlated with water use efficiency, and could be a good predictor for the WUE of forest

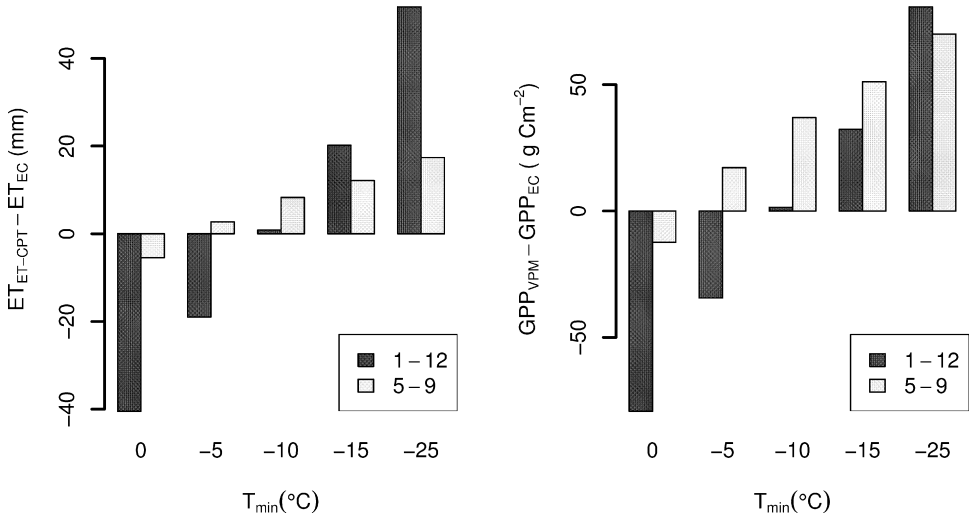

Fig. 10. Influence of T_{min} on annual (January 1 to December 31) and seasonal (May 1 to September 30) estimations of gross primary production and evapotranspiration. GPP_{EC} and ET_{EC} are measured gross primary production and evapotranspiration by eddy covariance method separately; GPP_{VPM}; ET_{ET-CPT} are predicted gross primary product and evapotranspiration, respectively.

ecosystem. Simulations of the ET-CPT model were conducted at 8-day intervals. The results have demonstrated the simple ET-CPT model has the potential to provide estimates of ET of forest-covered area with sufficient accuracy and timeliness for application in natural resource management services at large spatial scales.

Acknowledgements

This paper is a contribution to the ChinaFLUX projects at Changbai Mountains Forest Ecosystem Opened Research Station. This work was supported by the National Natural Science Foundation of China (No. 30590381, 30500079, 90411020). Xiao was supported by grants from NASA Land Use and Land Cover Change program.

References

Abbate, P.E., Dardanelli, J.L., Cantarero, M.G., Maturana, M., Melchiori, R.J.M., Suero, E.E., 2004. Climate and water availability effects on water-use efficiency in wheat. Crop Science 44, 474–483.

Allen, R.G., Tasumi, M., Morse, A., Trezza, R., 2005. A landsat-based energy balance and evapotranspiration model in Western US water rights regulation and planning. Irrigation and Drainage Systems 19, 251–268.

Baldocchi, D.D., Falge, E., Gu, L., Olson, R., Hollinger, D., 2001. FLUXNET: a new tool to study the temporal and spatial variability of ecosystem-scale carbon dioxide, water vapor and energy flux densities. Bulletin of the American Meteorological Society 82, 2415–2434.

Carlson, T.N., Buffum, M.J., 1989. On estimating total evapotranspiration from remote surface temperature measurements. Remote Sensing of Environment 29, 197–207.

Cleugh, H.A., Dunin, F.X., 1995. Modelling sensible heat fluxes from a wheat canopy: an evaluation of the resistance energy balance method. Journal of Hydrology 164, 127–152.

Cleugh, H.A., Leuning, R., Mu, Q., Running, S.W., 2007. Regional evaporation estimates from flux tower and MODIS satellite data. Remote Sensing of Environment 106, 285–304.

De Wit, C.T., 1958. Transpiration and Crop Yields. Versl. Landbouwk. Onderz. 64.6 Institute of Biological and Chemical Research on Field Crops and Herbage, Wageningen, The Netherlands, 88 pp.

Diao, Y., Wang, A., Jin, C., Guan, D., Pei, T., 2005. Simulation of evapotranspiration in broad-leaved and Korean pine mixed forest in Northeast China's Changbaishan Mountain using inverse Lagrangian dispersion analysis. Journal of Beijing Forestry University 27 (6), 29–351.

Garatuza-Payan, J., Watts, C.J., 2005. The use of remote sensing for estimating ET of irrigated wheat and cotton in NorthwestMexico. Irrigation and Drainage Systems 19, 301–320.

Gouranga, K., Harsh, N.V., 2007. Phenology based irrigation scheduling and determination of crop coefficient of winter maize in rice fallow of eastern India. Agricultural Water Management 75, 169–183.

Gutschick, V.P., 2007. Plant acclimation to elevated CO_2—from simple regularities to biogeographic chaos. Ecological Modelling 200, 433–451.

Hall, F., Huemmrich, F., Goetz, S.J., Sellers, P.J., Nikeson, J.E., 1992. Satellite remote sensing of surface energy balance: success, failures, and unresolved issues in FIFE. Journal of Geophysical Research 97, 19061–19089.

Hameed, T., Mario, M.A., 1993. Transfer function modeling if evapotranspiration modeling. In: Proceedings of the Conjucation on Management of Irrigation and Drain Systems: Integrated Perspectives, ASCE, New York, pp. 40–47.

Jiang, L., Islam, S., 2001. Estimation of surface evaporation map over Southern Great Plains using remote sensing data. Water Resources Research 37, 329–340.

Justice, C.O., Vermote, E., Townshend, J.R.G., Defries, R., Roy, D.P., Hall, D.K., Salomonson, V.V., Privette, J., Riggs, G., Strahler, A., Lucht, W., Myneni, R., Knjazihhin, Y., Running, S., Nemani, R., Wan, Z., Huete, A., van Leeuwen, W., Wolfe, R., 1998. The moderate resolution imaging radiospectrometer (MODIS): land remote sensing for global change research. IEEE Transactions on Geoscience and Remote Sensing 36, 1228–1249.

Kalma, J.D., Jupp, D.L.B., 1990. Estimating evaporation from pasture using infrared thermometry: evaluation of a one-layer resistance model. Agricultural and Forest Meteorology 51, 223–246.

Kustas, W.P., Norman, J.M., 1996. Use of remote sensing for evapotranspiration monitoring over land surface. IAHS Hydrological Sciences Journal 41, 495–516.

Law, B.E., Falge, E., Gu, L., Baldocchi, D.D., Bakwin, P., Berbigier, P., Davis, K., Dolman, A.J., Falk, M., Fuentes, J.D., Goldstein, A., Granier, A., Grelle, A., Hollinger, D., Janssens, I.A., Jarvis, P., Jensen, N.O., Katul, G., Mahli, Y., Matteucci, G., Meyers, T., Monson, R., Munger, W., Oechel, W., Olson, R., Pilegaard, K., Paw, U.K.T., Thorgeirsson, H., Valentini, R., Verma, S., Vesala, T., Wilson, K., Wofsy, S., 2002. Environmental controls over carbon dioxide and water vapor exchange of terrestrial vegetation. Agricultural and Forest Meteorology 113, 97–120.

Li, Z., Yu, G., Wen, X., Zhang, L., Ren, C., Fu, Y., 2005. Energy balance closure at ChinaFLUX sites. Sciences in China Series D: Earth Sciences 48 (Suppl. I), 51–62.

Limas, M.C., Ordieres Meré, J.B., Vergara González, E.P., Javier, F., 2007. AMORE: a MORE flexible neural network package. R Package Version 0.2–10. http://wiki.r-project.org/rwiki/doku.php?id=packages:cran:amore.

Mauser, W., Schädlich, S., 1998. Modelling the spatial distribution of evapotranspiration on different scales using remote sensing data. Journal of Hydrology 212–213, 250–267.

Moran, M.S., Rahman, A.F., Washburne, J.C., Goodrich, D.C., Weltz, M.A., Kustas, W.P., 1996. Combining the Penman–Monteith equation with measurements of surface temperature and reflectance to estimate evaporation rates of semiarid grassland. Agricultural and Forest Meteorology 80, 87–109.

Nagler, P.L., Cleverly, J., Glenn, E., Lampkin, D., Huete, A., Wan, Z., 2005a. Predicting riparian evapotranspiration from MODIS vegetation indices and meteorological data. Remote Sensing of Environment 94, 17–30.

Nagler, P.L., Scott, R.L., Westenburg, C., Cleverly, J.R., Glenn, E.P., Huete, A.R., 2005b. Evapotranspiration on western U.S. rivers estimated using the enhanced vegetation index from MODIS and data from eddy covariance and Bowen ratio flux towers. Remote Sensing of Environment 97, 337–351.

Nemani, R.R., Running, S.W., 1989. Estimation of regional surface resistance to evapotranspiration from NDVI and thermal-IR AVHRR data. Journal of Applied Meteorology 28, 276–284.

Potter, C.S., Randerson, J.T., Field, C.B., Matson, P.A., Vitousek, P.M., Mooney, H.A., Klooster, S., 1993. Terrestrial ecosystem production: a process model based on global satellite and surface data. Global Biogeochemical Cycles 7, 811–841.

Price, J.C., 1990. Using spatial context in satellite data to infer regional scale evapotranspiration. IEEE Xplore: Geoscience and Remote Sensing 28, 940–948.

Prince, S.D., Goward, S.N., 1995. Global primary production: a remote sensing approach. Journal of Biogeography 22, 815–825.

Raich, J.W., Rastetter, E.B., Melillo, J.M., Kicklighter, D.W., Steudler, P.A., Peterson, B.J., Grace, A.L., Moore III, B., Vorosmarty, C.J., 1991. Potential net primary production in South America: application of a global model. Ecological Application 1, 399–429.

Rana, G., Katerji, N., 2000. Measurement and estimation of actual evapotranspiration in the field under Mediterranean climate: a review. European Journal of Agronomy 13, 125–153.

Raupach, M.R., 2001. Combination theory and equilibrium evaporation. Quarterly Journal of the Royal Meteorological Society 127, 1149–1181.

Reichstein, M., Tenhunen, J.D., Roupsard, O., 2002. Severe drought effects on ecosystem CO_2 and H_2O fluxes at three Mediterranean evergreen sites: revision of current hypothesis? Global Change Biology 8, 999–1017.

Ruimy, A., Saugier, B., Dedieu, G., 1994. Methodology for the estimation of terrestrial net primary production from remotely sensed data. Journal of Geophysical Research 99, 5263–5283.

Running, S.W., Baldocchi, D.D., Turner, D., Gower, S.T., Bakwin, P., Hibbard, K., 1999. A global terrestrial monitoring network, scaling tower fluxes with ecosystem modeling and EOS satellite data. Remote Sensing of Environment 70, 108–127.

Schmid, H.P., 1994. Source areas for scalars and scalar fluxes. Boundary-Layer Meteorology 67, 293–318.

Scott, R., Edwards, E., Suttleworth, W., Huxmn, T., Watts, C., Goodrich, D., 2004. Interannual and seasonal variation in fluxes of water and carbon dioxide from a riparian woodland ecosystem. Agricultural and Forest Meteorology 122, 65–84.

Seguin, B., Courault, D., Gúerif, M., 1994. Surface temperature and evapotranspiration: application of local scale methods to regional scales using satellite data. Remote Sensing of Environment 49, 287–295.

Smith, R.C.G., Choudhury, B.J., 1990. Relationship of multispectral satellite data to land surface evaporation from the Australian continent. International Journal of Remote Sensing 11, 2069–2088.

Stanhill, G., 1986. Water use efficiency. Advance in Agronomy 39, 53–85.

Steduto, P., Katerji, N., Puertos-Molina, H., Ünlüa, M., Mastrorillic, M., Rana, G., 1997. Water-use efficiency of sweet sorghum under water stress conditions gas-exchange investigations at leaf and canopy scales. Field Crop Research 54, 221–234.

Tanner, C.B., Sinclair, T.R., 1983. Efficient water use in crop production: research or re-research? In: Taylor, H.M., Jordan, W.R., Sinclair, T.R. (Eds.), Limitations to Efficient Water Use in Crop Production. ASSA, CSSA, SSSA, Madison, WI, pp. 1–27.

Turner, D.P., Ritts, W.D., Cohen, W.B., Gower, S.T., Running, S.W., Zhao, M., Costa, M.H., Kirschbaum, A., Ham, J.M., Saleska, S.R., Ahl, D.E., 2006. Evaluation of MODIS NPP and GPP products across multiple biomes. Remote Sensing of Environment 102, 282–292.

Verstraeten, W.W., Veroustraete, F., Feyen, J., 2005. Estimating evapotranspiration of European forests from NOAA-imagery at satellite overpass time: towards an operational processing chain for integrated optical and thermal sensor data products. Remote Sensing of Environment 30, 256–276.

Wang, A., Jin, C., Guan, D., Pei, T., 2005. Application of inverse Lagrangian dispersion analysis in simulating forest evapotranspiration. Chinese Journal of Applied Ecology 16 (5), 843–848.

Wang, J., Miller, D.R., Sammis, T.W., Gutschick, V.P., Simmons, L.J., Andales, A.A., 2007. Energy balance measurements and a simple model for estimating pecan water use efficiency. Agricultural Water Management 91, 92–101.

Wilson, K., Goldstein, A., Falge, E., Aubinet, M., Baldocchi, D., Berbigier, P., Bernhofer, Ch., Ceulemans, R., Dolman, H., Field, C., Grelle, A., Law, B., Meyers, T., Moncrieff, J., Monson, R., Oechel, W., Tenhunen, J., Valentini, R., Verma, S., 2002. Energy balance closure at FLUXNET sites. Agricultural and Forest Meteorology 113, 223–243.

Wofsy, S.C., Goulden, M.L., Munger, J.W., Fan, S.M., Bakwin, P.S., 1993. Net exchange of CO_2 in a mid-latitude forest. Science 260, 1314–1317.

Wu, J., Guan, D., Zhang, M., Han, S., Jin, C., 2005. Comparison of eddy covariance and BREB methods in determining forest evapotranspiration: case study on broad-leaved Korean pine forest in Changbai Mountain. Chinese Journal of Ecology 24 (10), 1245–1249.

Wylie, B., Johnson, D., Laca, E., Saliendra, N., Gilmanov, T., Reed, B., 2003. Calibration of remotely sensed, coarse resolution NDVI to CO_2 fluxes in a sage-brush-steppe ecosystem. Remote Sensing of Environment 85, 243–255.

Xiao, X., Braswell, B., Zhang, Q., Boles, S., Frolking, S., Moore III, B., 2003. Sensitivity of vegetation indices to atmospheric aerosols: continental-scale observations in Northern Asia. Remote Sensing of Environment 84, 385–392.

Xiao, X., Hagen, S., Zhang, Q., Keller, M., Moore, B., 2006. Detecting leaf phenology of seasonally moist tropical forests in South America with multi-temporal MODIS images. Remote Sensing of Environment 103, 465–473.

Xiao, X., Hollinger, D., Aber, J.D., Goltz, M., Davidson, E.A., Zhang, Q.Y., 2004a. Satellite-based modeling of gross primary production in an evergreen needle-leaf forest. Remote Sensing of Environment 89, 519–534.

Xiao, X., Zhang, Q., Braswell, B., Urbanski, S., Boles, S., Wofsy, S.C., Moore, B.I., Ojima, D., 2004b. Modeling gross primary production of a deciduous broadleaf forest using satellite images and climate data. Remote Sensing of Environment 91, 256–270.

Xiao, X., Zhang, Q., Hollinger, D., Aber, J., Moore, B., 2005. Modeling gross primary production of an evergreen needleleaf forest using MODIS and climate data. Ecological Applications 15, 954–969.

Yang, X., Zhou, Q., Melville, M., 1997. Estimating local sugarcane evapotranspiration using Landsat TM image and a VITT concept. International Journal of Remote Sensing 18, 453–459.

Yu, G.R., Song, X., Wang, Q., Liu, Y., Guan, D., Yan, J., Sun, X., Zhang, L., Wen, X., 2008. Water-use efficiency of forest ecosystems in eastern China and its relations to climate variables. New Phytologist 177, 927–937.

Zhang, J., Han, S., Sun, X., Tang, F., 2005. UU* filtering of nighttime net ecosystem CO_2 exchange flux over forest canopy under strong wind in wintertime. Sciences in China Series D: Earth Sciences 48 (Suppl. I), 85–92.

Zhang, J., Han, S., Yu, G., 2006a. Seasonal variation in carbon dioxide exchange over a 200-year-old Chinese broad-leaved Korean pine mixed forest. Agricultural and Forest Meteorology 137, 150–165.

Zhang, J., Yu, G., Han, S., Guan, D., Sun, X., 2006b. Seasonal and annual variation of CO_2 flux above a broadleaved Korean pine mixed forest. Sciences in China Series D: Earth Sciences 49 (Suppl. I), 60–69.